JOURNAL OF THE KOREAN ASTRONOMICAL SOCIETY
38: 69 ~ 72, 2005

FUV IMAGING SPECTROSCOPIC OBSERVATIONS OF INTERSTELLAR MEDIUM WITH FIMS

KWANG-IL SEON[1], WONYONG HAN[1], DAE-HEE LEE[1], UK-WON NAM[1], JANG-HYUN PARK[1], IN-SOO YUK[1], HO JIN[1], KYUNG WOOK MIN[2], KWANG-SUN RYU[2], JERRY EDELSTEIN[3], AND ERIC KORPELA[3]
[1]Korea Astronomy and Space Science Institute, 61-1 Hwaam-dong Yuseong-gu, Daejeon, 305-348
E-mail: kiseon@kasi.re.kr
[2]Korea Advanced Institute of Science and Technology, 373-1 Guseong-dong Yuseong-gu, Daejeon, 305-701
[3]Space Sciences Laboratory, University of California, Berkeley, CA 947620-7450, USA
(Received February 1, 2005; Accepted March 15, 2005)

ABSTRACT

The FIMS (Far-ultraviolet IMaging Spectrograph; also known as SPEAR, Spectroscopy of Plasma Evolution from Astrophysical Radiation) is the primary payload of the STSAT-1, the first Korean science satellite, which was launched in September, 2003. The FIMS performs spectral imaging of diffuse far-ultraviolet emission with the unprecedented wide field of view and the relatively good spectral resolution. We present far-ultraviolet spectral observations of highly ionized interstellar medium including supernova remnants, superbubbles, soft X-ray shadows, and the molecular hydrogen fluorescent emission lines. The FIMS has detected He II, C III, O III], O IV, Si IV, O VI, and H_2 fluorescent emission lines. The emission lines arise in shocked or thermally heated and in photo-ionized gases. We present an overview of the FIMS instrument and its initial observational results.

Key words : instrumentation: spectrographs — ISM: supernova remnants — ISM: molecules — ISM: bubbles — ultraviolet: ISM

I. INTRODUCTION

The FIMS (Far-ultraviolet IMaging Spectrogaph, also known as SPEAR) space mission, launched in late 2003, has conducted the first large-scale spectral mapping of cosmic far ultraviolet (FUV, 900–1750 Å) emission (Edelstein et al. 2003). The primary scientific objectives of FIMS are 1) to trace the energy flow through the hot plasma found on scales ranging from supernova bubbles to galaxies and galactic coronae, 2) to map the distribution of the local and global structures of hot plasma, and 3) to investigate the earth aurora at various FUV wavelengths. FIMS is the primary payload on the first Korean Science and Technology SATellite (STSAT-1). The FIMS system has developed by a joint research project of KASI, KAIST and U. C. Berkeley.

The FIMS's broad bandpass ($\lambda\lambda 900 - 1750$Å), spectral resolution ($\lambda/\delta\lambda \sim 500$), large field of view ($7.4^\circ \times 4.5'$), and imaging resolution ($\sim 10'$) were chosen to facilitate the measurement of the ionization, temperature, and depletion of energetic interstellar gas while rejecting airglow emission and stellar contamination that have plagued earlier measurements attempts. The bandpass is designed for useful spectral diagnostics of plasma with characteristic temperatures of 10^4 K – 10^6 K. In this paper, we present an overview of the instrument and its initial observational results to demonstrate the quality of FIMS data. Detailed descriptions on the individual topics will be published elsewhere.

Proceedings of *the 6th East Asian Meeting of Astronomy*, held at Seoul National University, Korea, from October 18-22, 2004.

II. INSTRUMENTS

The FIMS instrument consists of dual imaging spectrographs optimized for the detection of faint diffuse radiation. The two spectral channels are designated as the "short" ($\lambda\lambda 900 - 1175$Å) and "long" ($\lambda\lambda 1335 - 1750$Å) bandpasses. The bandpass scheme was chosen to include a variety of astrophysically important emission lines from abundant ionic species while avoiding intense geocoronal line contamination from H Lyman 1216Å and O I 1304Å radiation. Each spectrograph channel consists of a collecting mirror feeding a slit, a diffraction grating and detector. The each channel uses identically figured 5×8 cm^2 elements in the same geometric configuration and shares the same slit and detector focal plane.

The unique two-element f/2.2 optical system uses a cylindrical parabolic collecting mirror that focuses plane-parallel light from infinity to a slit (see Fig. 1). The cylindrical wave from the slit illuminates an ellipse of rotation surface with constant grating rulings that focuses an imaged spectrum to a position sensitive detector. Radiation from off-plane angles is imaged along the detector perpendicular to the dispersion plane, analogous to a slit-imaging spectrograph. The optical surface parameters were selected to correct on-axis aberrations to the third order using an analytical approximation that was refined with numerical raytracing. The cylindrical-source scheme was chosen because it doubles the usable imaging angle in comparison

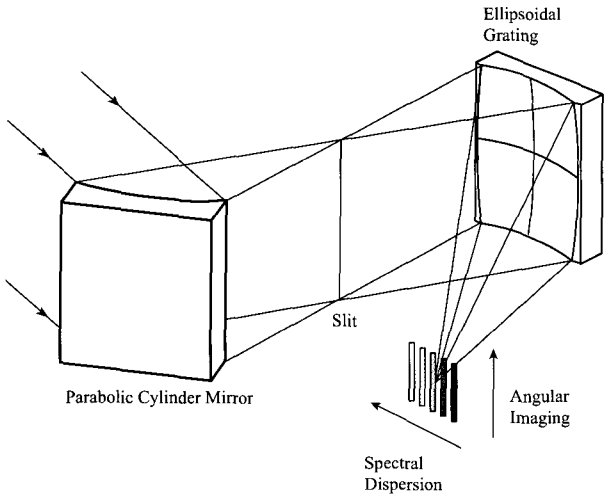

Fig. 1.— Optical concept of FIMS.

with classical point-source spectrographs. The result is a large solid angle and collecting area product, a determining factor for diffuse source sensitivity. The FIMS design is derived from the two flight-proven EURD instruments (Bowyer, Edelstein, & Lampton 1997). The imaging performance allows for a large field with imaging resolution similar to other important interstellar all-sky surveys. Monte-Carlo simulation has been performed to verify the detection sensitivity of O VI and C IV emission lines, which are brightest emission lines predicted to occur in galactic plasma cooling models (Seon et al. 2000). A parabolic cylindrical mirror has been manufactured in Korea (Ryu et al. 2003).

Each channel's spectrum is focused upon a separate position-sensitive photon-counting microchannel plate (MCP) stack. The MCPs are coated with a CsI and KBr photocathodes. The stacks share a single position-sensitive read-out and electronics system to conserve spacecraft resources. The unique detector read-out uses a cross delay line anode system with one bifurcated delay line that senses both channel stacks (Nam et al. 2003). The axes of the anode are rotated 15 degrees with respect to the dispersion axis to mitigate the appearance of false spectral features due to anode or electronics differential non-linearity. A stimulation unit injects artificial event signals at the field corners so that thermal drifts in the position encoding system can be calibrated in flight. The amplifiers also produce a signal proportional to each event's charge amplitude to allow the rejection of low amplitude noise or high amplitude ion and cosmic ray events. A count-rate monitor turns off the detector in case of excessive count-rates. Observation restart is automatically attempted within 2 to 30 s so that entire survey sweeps will not be lost while momentary bright stars transits.

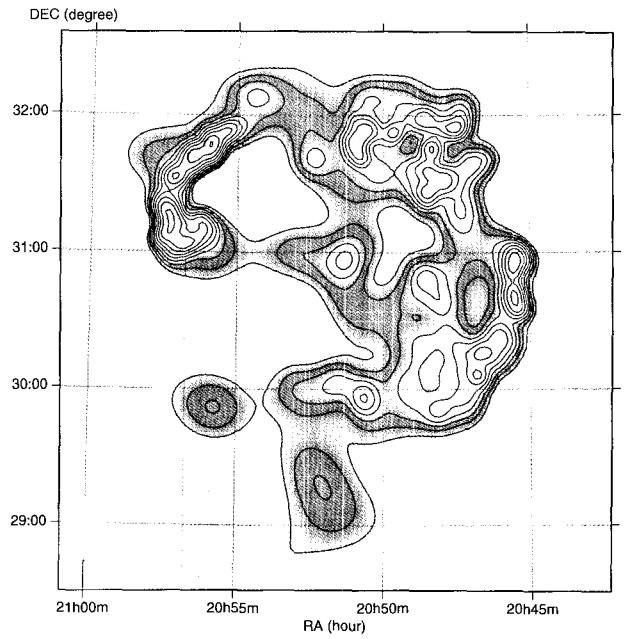

Fig. 2.— C IV emission map of Cygnus Loop observed with FIMS. The image was adaptively smoothed.

III. PRELIMINARY RESULTS

(a) Supernova Remnant: Cygnus Loop

The Cygnus Loop is the prototypical middle-aged supernova remnant. The Cygnus Loop shows a limb-brightened morphology at X-ray, optical, infrared (IR), and radio wavelengths (Ku et al. 1984; Charles, Kahn, & McKee 1985; Braun & Strom 1986; Fesen, Blair, & Kirshner 1982; Keen et al. 1973). Because of its proximity, large angular size, relatively low reddening, and its brightness, it has been extensively studied in the UV with IUE, Voyager, the HUT, the HST, and the FUSE. Global aspects of the ultraviolet emission have been studied by Rasmussen & Martin (1992), and Blair et al. (1991), mainly focused on the O VI emission lines. Blair et al. (1991) have produced skymaps with nearly complete coverage of the Cygnus Loop using a large set of the Voyager data, in two of the available UV emission lines, measured at λ980 and λ1036. They showed that the 980Å feature arises mainly from regions of bright optical emission, whereas the 1035Å emission more closely resembles the X-ray emission. However, the overall morphology of the Cygnus Loop at the rather longer ultraviolet emission lines, such as at C IV (λ1550Å), has never been measured.

In Fig. 2, we show the spectral image of C IV emission line. The spectral map is smoothed with an adaptive smoothing algorithm. Their spatial distributions are generally that of a limb-brightened shell, and similar to soft X-ray maps. The spectral lines He II (λ1640), O III (λ1664), and O IV]+Si IV (λ1400) were also detected.

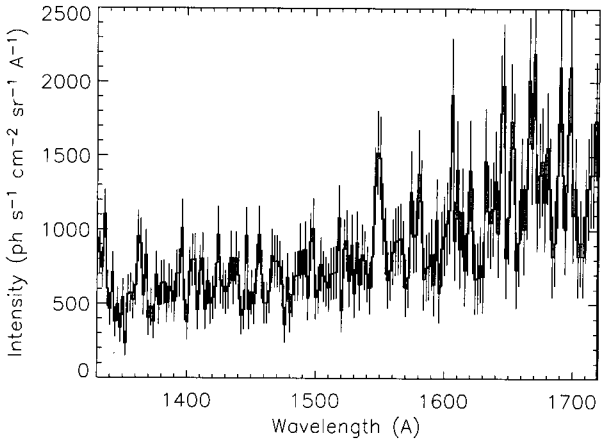

Fig. 3.— FUV spectrum of an X-ray shadow direction observed with FIMS. Uncertainties are also shown. C IV (λ1550Å) emission line is clearly shown.

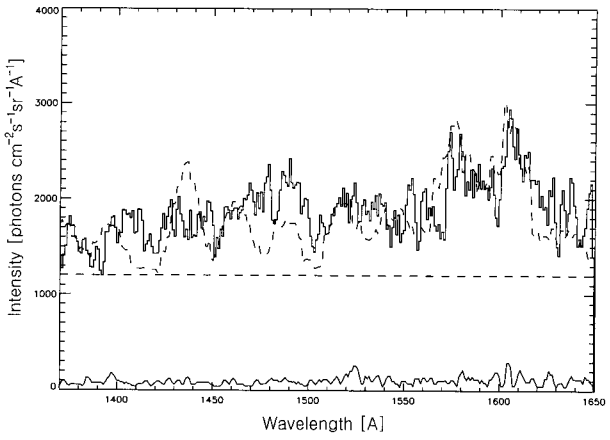

Fig. 4.— FUV spectrum of the Taurus cloud observed with FIMS. Overplotted dashed spectrum is CLOUD fitting result. Calculated uncertainties are shown below.

(b) Soft X-ray Shadows

A negative correlation between the column density distribution of a Galactic H I feature and the surface brightness of the soft X-ray diffuse background (SXRB), "shadow", provides a mechanism for determining the location along the line of sight of X-ray-emitting plasmas relative to the X-ray-absorbing H I.

Shadows in the general SXRB (i.e., away from discrete emission features such as supernova remnants) were first unambiguously detected using the ROSAT observatory (Snowden et al. 1991). The continuing study of such shadows has provided crucial information about the soft X-ray emission from the Galactic halo and from the Local Hot Bubble (LHB), an irregularly shaped region of $\sim 10^6$ K plasma that extends $\sim 50 - 150$ pc from the Sun in all directions (Cox & Snowden 1986; Cox & Reynolds 1987; Snowden et al. 1998).

Snowden et al. (2000) compiled a catalog of soft X-ray shadows extensively. This paper investigates the lines of sight compiled by them and by Snowden et al. (1998). All photon events from the soft X-ray shadows whose line of sights are known from the literatures were extracted from FIMS observation database. We detected the C IV resonance line emission ($\lambda\lambda$ 1548, 1551) and other emission lines originating from the soft X-ray shadows using the spectroscopic data obtained with the FIMS. Fig. 3 shows an example spectrum observed toward an X-ray shadow direction. The emission lines from the hot ISM in Local Bubble will be studied through careful investigation.

(c) Molecular Hydrogen

Molecular clouds are the birthplace of stars, and the newly born stars radiate intense ultraviolet photons which govern the chemical and the physical properties of the nearby molecular clouds. H_2 molecules which absorb FUV photons in the Lyman ($B^1\Sigma_u^+ - X^1\Sigma_g^+$) and Werner ($C^1\Pi^u - X^1\Sigma_g^+$) bands are electronically excited. Subsequent fluorescence leads to dissociation of the H_2 molecules in about 10% of the cases ,or to H_2 molecules in vibrationally excited states of the ground electronic state in the remaining 90% of the cases (Black & Dalgarno 1976; Seon et al. 2003).

When the fluorescent transitions from the electronically excited state to the various vibration-rotation states in the electronic ground state occur on the time scale of 10^{-8} sec, FUV lines in the Lyman and Werner bands are emitted. Since the FUV band data are only accessible from the space telescope, a few observations of these H_2 emission have been reported, e.g., the reflection/emission nebula IC 63, the diffuse interstellar medium, the pre-main-sequence star T Tauri and Burnham's nebula, the Herbig-Haro objects HH 43 and HH 47, and Jupiter's aurora (see Seon et al. 2003 for the references).

The FIMS provides the first survey opportunity for the observation of H_2 fluorescence lines. FUV ($1370 - 1630$Å) emissions from the Taurus cloud region was observed with FIMS. The FUV image reveals the Taurus cloud has a filamentary structure with a typical width of 1 pc. H_2 model CLOUD fitting (van Dishoeck & Black 1988) is well matched when cloud density n(H) = 50 cm^{-3} and incident UV intensity $I_{UV} = 0.4$ with different optical depth for each region. Both H_2 fluorescence and dust scattered starlight in FUV suffer self-shielding when the optical depth becomes higher. A comparative study on the various images of the Taurus region, such as the extinction map, $I_{100\mu m}$ and $I_{60\mu m}$ emission images, and FUV emission image, results that all three emissions are coming from different depth of a cloud, in order of wavelength along the cloud depth. Fig. 4 shows a FUV spectrum of the Taurus cloud observed with FIMS.

We also have detected H_2 fluorescence lines in the

Eridanus region for the first time with the FIMS instrument. The comparisons with model predictions show that the spectral features are not only the consequence of the photon excitation on molecular clouds but also of the heating and excitation by the shocks passing the region. According to the spectrum analysis and emission model studies, the FUV emission of H_2 molecules from the Eridanus supershell implies the preexisting molecular clouds in the region are swept and heated by interstellar shocks up to $\sim 2,000 \pm 1,100$ K and then are being exposed to strong radiation field from the Orion O/B association.

IV. SUMMARY

The FIMS space mission, launched in late 2003, has performed the first large-scale spectral mapping of cosmic far ultraviolet (FUV, 900–1750 Å) emission. We presented initial analysis results of the supernova remnant, Cygnus Loop, H_2 molecular fluorescent emission regions, the Taurus cloud and the Eridanus supershell, and the X-ray shadows. We have detected He II, C III, O III], O IV, Si IV, O VI, and H_2 fluorescent emission lines from the targets. These FIMS data allow us to study the hot and cold interstellar mediums on both large and small scales.

ACKNOWLEDGEMENTS

FIMS/SPEAR is a joint project of the Korea Astronomy and Space Science Institute, Korea Advanced Institute of Science and Technology, and University of California at Berkeley, funded by the Ministry of Science and Technology of Korea and National Aeronautics and Space Administration.

REFERENCES

Black, J. H., & Dalgarno, A., 1976, ApJ, 203, 132

Blair, W. P., Long, K. S., Vancura, O., & Holberg, J. B., 1991, ApJ, 374, 202

Bowyer, S., Edelstein, J.,.& Lampton, M., 1997, ApJ, 485, 523

Braun, R., & Strom, R. G., 1986, A&A, 164, 193

Charles, P. A., Kahn, S. M., & McKee, C. F., 1985, ApJ, 295, 456

Cox, D. P., & Reynolds, R. J., 1987, ARA&A, 25, 303

Cox, D. P., & Snowden, S. L., 1986, Adv. Space Res., 6, 97

Edelstein, J., Korpela, E., Welsh, B., Min, K.-W., Han, W., & Nam, U.-K., 2003, Proc. of SPIE, 4854, 329

Fesen, R. A., Blair, W. P., & Kirshner, R. P., 1982, ApJ, 262, 171

Keen, N. J., Wilson, W. E., Haslam, C. G. T., Graham, D. A.,

& Thomasson, P., 1973, A&A, 28, 197

Ku, W. H.-M., Kahn, S. M., Pisarski, R., & Long, K. S., 1984, ApJ, 278, 615

Nam, U.-W., Rhee, J.-G., Korpela, E., Jin, H., Lee, D.-Hee, Hull, J.,

Berg, P., Han, W., Min, K.-W., & Edelstein, J., 2003, Proc. of SPIE, 4854, 602

Rasmussen, A., & Martin, C., 1992, ApJ, 396, L103

Ryu, K.-S., Nishikida, K., Edelstein, J., Seon, K.-I., Yuk, I.-S.,

Min, K.-W., Han, W., Korpela, E., Chung, R., & McKee, K., 2003, Proc. of SPIE,

4854, 457

Seon, K.-I., Park, S.-J., Park, J.-H., Yuk, I.-S., Jin, H., Nam, U.-K., Han, W.,

Ryu, K.-S., Lee, D.-H., Oh, S.-H., Park, Y.-S., Korpela, E., Edelstein, J., Nishikida, K.,

Shinn, J.-H., Rhee, J.-G., Min, K.-W., & Kim, Y.-H., 2003, JKPS, 43, 565

Seon, K.-I., Ryu, K.-S., Yuk, I.-S., Park, J.-H., Nam, U.-W., Han, W.,

Seon, J.-H., Min, K.-W., Edelstein, J., & Korpela, E., 2000, JASS, 17, 77

Snowden, S. L., Egger, R., Finkbeiner, D. P., Freyberg, M. J., & Plucinsky, P. P., 1998, ApJ, 493, 715

Snowden, S. L., Freyberg, M. J., Kuntz, K. D., & Sanders, W. T., 2000, ApJ, 128, 171

Snowden, S. L., Mebold, U., Hirth, W., Herbstmeier, U., & Schmitt, J. H. M. M., 1991, Science, 252, 1529

van Dishoeck, E. F., & Black, J. H., 1988, ApJ, 334, 771